



ATLAS Note
GROUP-2017-XX
2nd September 2020



1

2

3

EFT Interpretations of $t\bar{t}H$ Production in Multilepton Final States at $\sqrt{s} = 13$ TeV

4

The ATLAS Collaboration

5

6

7

8

9

10

11

The possibility of using the kinematic properties of the Higgs boson to search for new physics is investigated using $t\bar{t}H$ events with multiple leptons in the final state. A deep neural-network is used to reconstruct the momentum spectrum of the Higgs, which would be altered by the presence of new physics without affecting the overall rate of $t\bar{t}H$ production. Simulations representing 139 fb^{-1} at $\sqrt{s} = 13$ TeV are used to place expected limits on physics 'beyond the Standard Model' affecting the coupling of the Higgs boson to the top quark.

¹⁴ **Contents**

¹⁵ **1 Changes and outstanding items**

¹⁶ **1.1 Changelog**

¹⁷ This is version 1

2 Introduction

Since the discovery of a Higgs boson compatible with the Standard Model (SM) in 2012 [], its interactions with other particles have been studied using proton-proton collision data produced by the Large Hadron Collider (LHC). The strongest of these interactions is the coupling of the Higgs to the top quark, making the Yukawa coupling between these two particles of particular interest for study.

These interactions can be measured directly by studying the production of a Higgs Boson in association with a pair of Top Quarks ($t\bar{t}H$) []. While this process has been observed by both the ATLAS [] and CMS [] collaborations, these analyses have focused on measuring the overall rate of $t\bar{t}H$ production. There are several theories of physics Beyond the Standard Model (BSM), however, that would affect the kinematics of $t\bar{t}H$ production without altering its overall rate [].

An Effective Field Theory approach can be used to model the low energy effects of new, high energy physics, by parameterizing BSM effects as dimension-six operators. The addition of these operators can be shown to modify the transverse momentum (p_T) spectrum of the Higgs Boson []. Therefore, reconstructing the momentum spectrum of the Higgs provides a means to observe new physics in the Higgs sector.

This note reports on the feasibility of measuring the impact of dimension-six operators in $t\bar{t}H$ events with multiple leptons in the final state, using Monte Carlo (MC) simulations scaled to 139 fb^{-1} at an energy $\sqrt{s} = 13 \text{ TeV}$. Events are separated into channels based on the number of light leptons (electrons and muons) in the final state - either two same-sign leptons (2LSS), or three leptons (3L). A deep neural network is used to identify which objects originate from the decay of the Higgs, and reconstruct the momentum of the Higgs Boson in each event. This reconstructed momentum spectrum is used to place limits on BSM effects, and on the parameters of dimension-six operators.

This note is organized as follows: Section ?? describes the LHC and the ATLAS detector. The dataset and Monte Carlo (MC) simulations used in the analysis is outlined in section ?. Section ?? describes the identification and reconstruction of the various physics objects. The models used to reconstruct the momentum spectrum of the Higgs is discussed in section ?. The selection and categorisation of events comprises section ?, and the theoretical and experimental systematic uncertainties considered are described in section ?. Finally, the results of the study are summarized in section ?.

3 The ATLAS Detector

ATLAS is a general purpose detector designed to maximize the detection efficiency of nearly all physics objects, including leptons, jets, and photons, while covering nearly the entire solid angle around the collision point. Just surrounding the interaction point is the Inner Detector, designed

to track the path of charged particles moving through the detector. An inner solenoid surrounding the Inner Detector is used to produce a magnetic field of 2 T.

The Inner Detector consists of three components - the Pixel Detector, the Semi-Conductor Tracker (SCT), and the Transition Radiation Tracker (TRT). The Pixel Detector is the innermost of these, beginning just 33.25 mm away from the beam line. It consists of three silicon layers along the barrel, as well as three endcap layers, covering a range of $|\eta| < 2.5$. The Semiconductor Tracker (SCT) is similar to the Pixel detector, but uses long strips rather than small pixel to cover a larger spatial area.

Situated outside the Inner Detector are two concentric calorimeters, covering a range of $|\eta| < 4.9$. The inner calorimeter uses liquid argon (LAr) to measure energy of particles that interact electromagnetically within the region $|\eta| < 3.2$, and consists of around 180,000 readout channels. The outer calorimeter, or hadronic calorimeter, is composed of steel plates, with scintillating tiles as the active material. It covers a range of $|\eta| < 1.7$, and the signals from the hadronic calorimeter are read out by photomultiplier tubes (PMTs). The remaining pseudorapidity range is covered by forward calorimeter modules.

The outermost layer of the detector, the muon spectrometer, consists of tracking and triggering system. It extends from the outside of the calorimeter system, about a 4.25 m radius from the beam line, to a radius of 11 m. Two large toroidal magnets within the muon system generate a large magnetic ranging between 2 T and 8 T. 1200 tracking chambers are placed in the muon system in order to precisely measure the tracks of muons within $|\eta| < 2.7$ with high spatial resolution.

A two-level trigger system is used to select out events to be recorded. The level-1 trigger uses hardware information from the calorimeters and muon spectrometer to select events that contain candidates for particles commonly used in analysis, and reduces the rate of events from 40 MHz to around 100 kHz. Events that pass the level-1 trigger move to the High-Level Trigger (HLT). The HLT takes place outside of the detector in software, and looks for properties such as a large amount of missing transverse energy, well defined leptons, and multiple high energy jets. Events that pass the HLT are stored and used for analysis. Because the specifics of the HLT are determined by software rather than hardware, the thresholds can be changed throughout the run of the detector in response to run conditions such as changes to pileup and luminosity. After the HLT is applied, the event rate is reduced to around 1 kHz, which are recorded for analysis.

4 Data and Monte Carlo Samples

This study used data collected by the ATLAS detector over the period from 2015-2018, representing 138.9 fb⁻¹ of data at an energy of 13 TeV.

Several Monte Carlo generators were used to simulate both signal and background processes. For all of these, the effects of the ATLAS detector are simulated in Geant4.

5 Object Reconstruction

Events are required to be selected by dilepton triggers, as summarized in table ??.

Dilepton triggers (2015)	
$\mu\mu$ (asymm.)	HLT_mu18_mu8noL1
ee (symm.)	HLT_2e12_lhloose_L12EM10VH
$e\mu, \mu e$ (~symm.)	HLT_e17_lhloose_mu14
Dilepton triggers (2016)	
$\mu\mu$ (asymm.)	HLT_mu22_mu8noL1
ee (symm.)	HLT_2e17_lhvloose_nod0
$e\mu, \mu e$ (~symm.)	HLT_e17_lhloose_nod0_mu14
Dilepton triggers (2017)	
$\mu\mu$ (asymm.)	HLT_mu22_mu8noL1
ee (symm.)	HLT_2e24_lhvloose_nod0
$e\mu, \mu e$ (~symm.)	HLT_e17_lhloose_nod0_mu14
Dilepton triggers (2018)	
$\mu\mu$ (asymm.)	HLT_mu22_mu8noL1
ee (symm.)	HLT_2e24_lhvloose_nod0
$e\mu, \mu e$ (~symm.)	HLT_e17_lhloose_nod0_mu14

Table 1: List of lowest p_T -threshold, un-prescaled dilepton triggers used for 2015-2018 data taking.

Electron candidates are reconstructed from energy clusters in the electromagnetic calorimeter that are associated with charged particle tracks reconstructed in the inner detector [ATLAS-CONF-2016-024].

Electron candidates are required to have $p_T > 10$ GeV and $|\eta_{\text{cluster}}| < 2.47$. Candidates in the transition region between different electromagnetic calorimeter components, $1.37 < |\eta_{\text{cluster}}| < 1.52$, are rejected. A multivariate likelihood discriminant combining shower shape and track information is used to distinguish real electrons from hadronic showers (fake electrons). To further reduce the non-prompt electron contribution, the track is required to be consistent with originating from the primary vertex; requirements are imposed on the transverse impact parameter significance ($|d_0|/\sigma_{d_0}$) and the longitudinal impact parameter ($|\Delta z_0 \sin \theta_\ell|$), as shown in table ??.

Muon candidates are reconstructed by combining inner detector tracks with track segments or full tracks in the muon spectrometer [PERF-2014-05]. Muon candidates are required to have $p_T > 10$ GeV and $|\eta| < 2.5$. All leptons are required to be isolated, and pass a non-prompt BDT selection described in detail in [ttH_paper].

Jets are reconstructed from calibrated topological clusters built from energy deposits in the calorimeters [ATL-PHYS-PUB-2015-015], using the anti- k_t algorithm with a radius parameter $R = 0.4$. Jets with energy contributions likely arising from noise or detector effects are removed

from consideration [ATLAS-CONF-2015-029], and only jets satisfying $p_T > 25$ GeV and $|\eta| < 2.5$ are used in this analysis. For jets with $p_T < 60$ GeV and $|\eta| < 2.4$, a jet-track association algorithm is used to confirm that the jet originates from the selected primary vertex, in order to reject jets arising from pileup collisions [PERF-2014-03].

Missing transverse momentum (E_T^{miss}) is used as part of the event selection. The missing transverse momentum vector is defined as the inverse of the sum of the transverse momenta of all reconstructed physics objects as well as remaining unclustered energy, the latter of which is estimated from low- p_T tracks associated with the primary vertex but not assigned to a hard object [ATL-PHYS-PUB-2015-027].

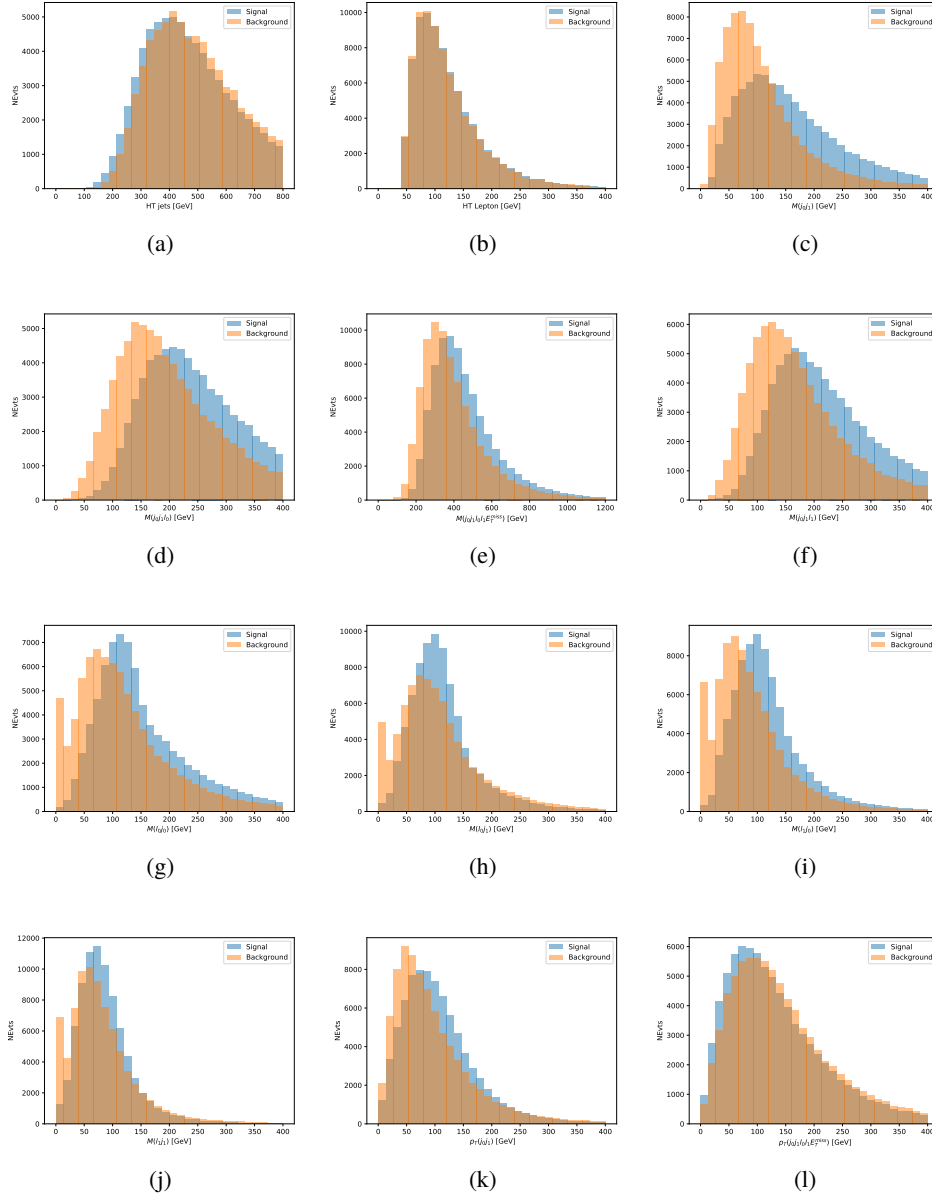
6 Higgs Momentum Reconstruction

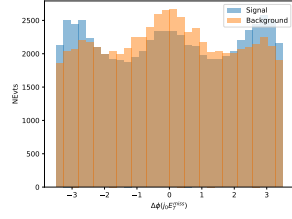
Reconstructing the momentum of the Higgs boson is a particular challenge for channels with leptons in the final state: Because all channels include at least two neutrinos in the final state, the Higgs can never be fully reconstructed. However, the momentum spectrum can be well predicted by a neural network when provided with the four-vectors of the Higgs Boson decay products, as shown in section ???. With this in mind, a sophisticated approach involving several layers of MVAs is used to reconstruction the Higgs momentum.

The first layer is a Neural Network designed to select which jets are most likely to be the b-jets that came from the top decay. The kinematics of these jets are fed into the second layer, also a BDT, which is designed to identify the decay products of the Higgs Boson itself. The kinematics of these particles are then fed into a deep neural-network, which predicts the momentum of the Higgs.

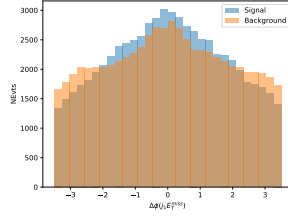
6.1 Truth Level Reconstruction

Reconstructed physics objects are matched to truth

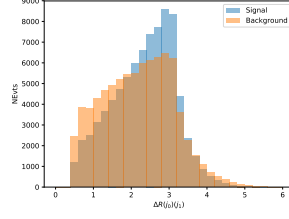




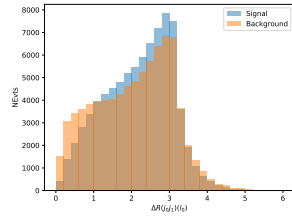
(m)



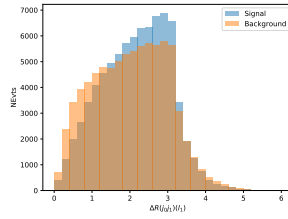
(n)



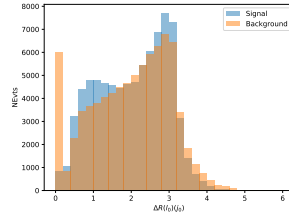
(o)



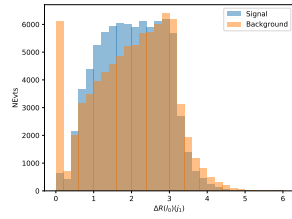
(p)



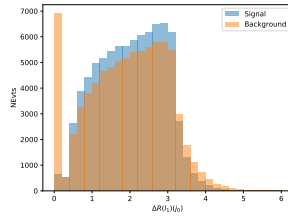
(q)



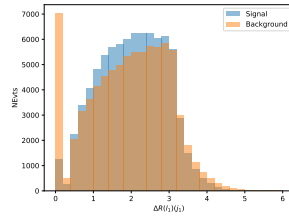
(r)



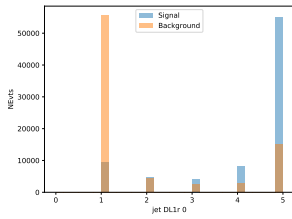
(s)



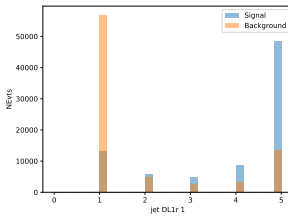
(t)



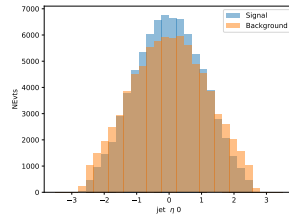
(u)



(v)



(w)



(x)

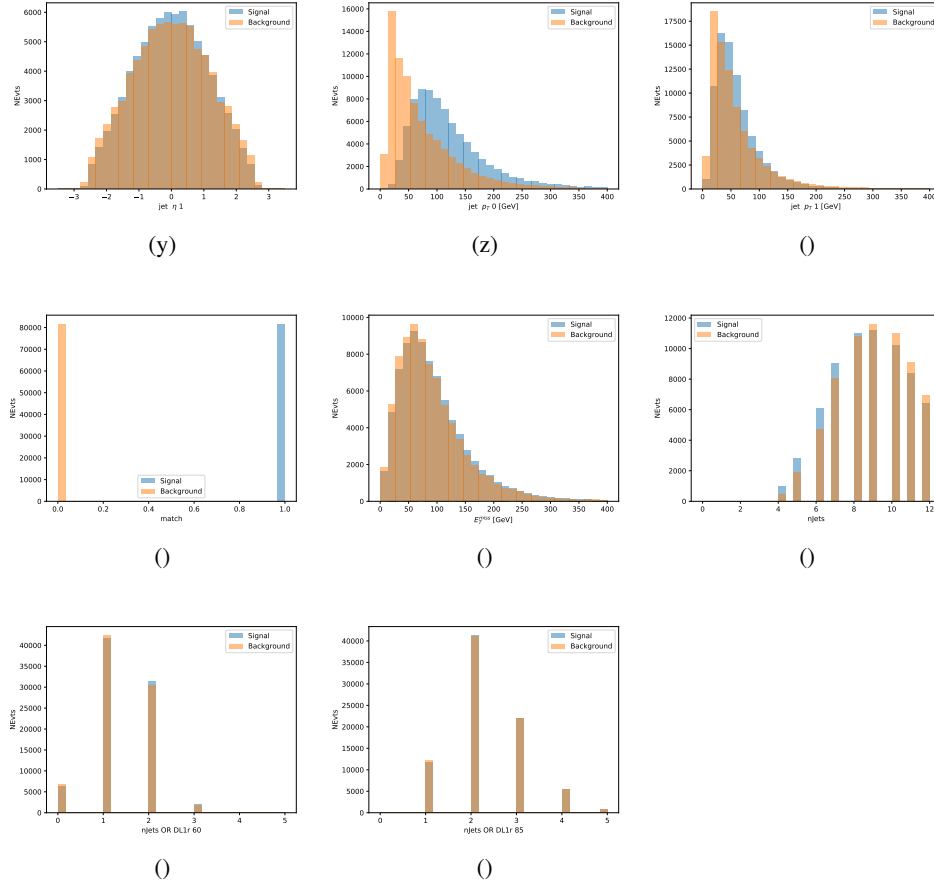


Figure 6.1: Input features for top2lSS training

129 6.2 b-jet Identification

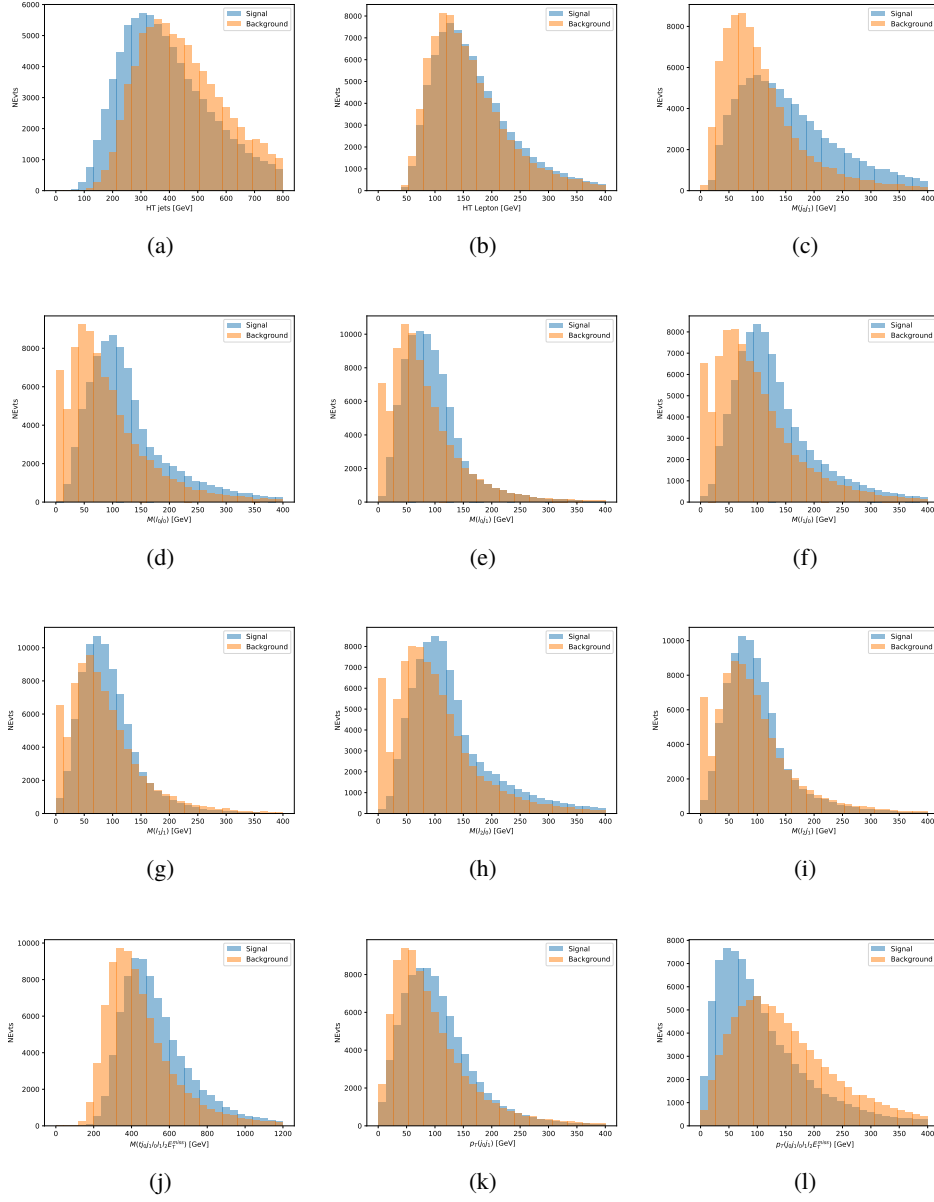
130 6.3 Higgs Reconstruction

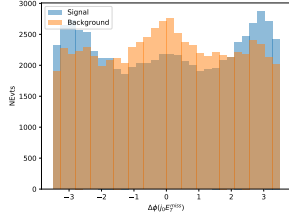
131 6.4 p_T Prediction

132 6.5 3l Decay Mode

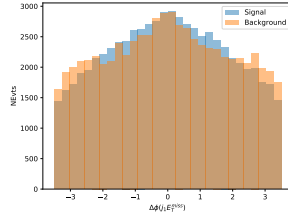
133 7 Signal Region Definitions

134 Events are divided into two channels based on the number of leptons in the final state: one with
 135 two same-sign leptons, the other with three leptons. The 3l channel includes events where both
 136 leptons originated from the Higgs boson as well as events where only one of the leptons

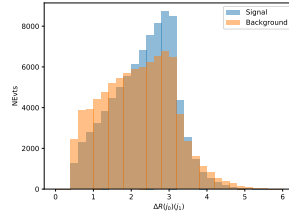




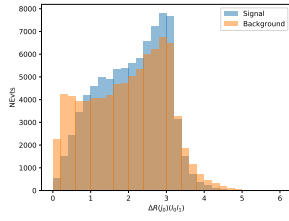
(m)



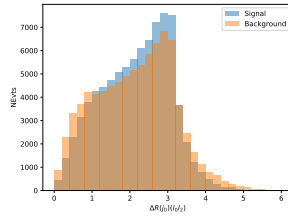
(n)



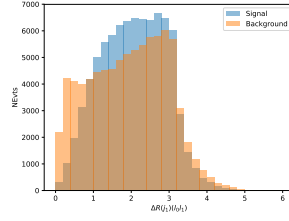
(o)



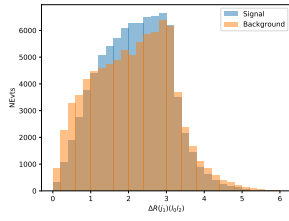
(p)



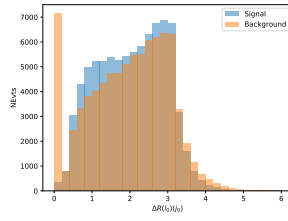
(q)



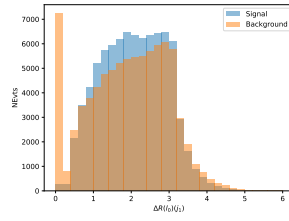
(r)



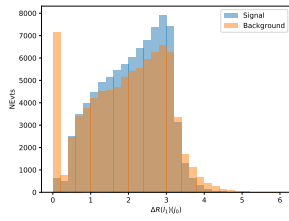
(s)



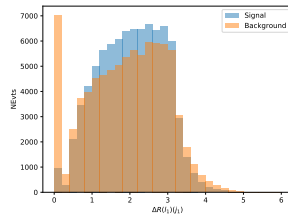
(t)



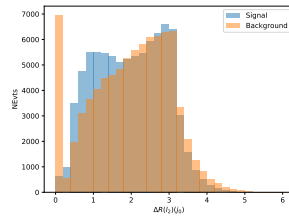
(u)



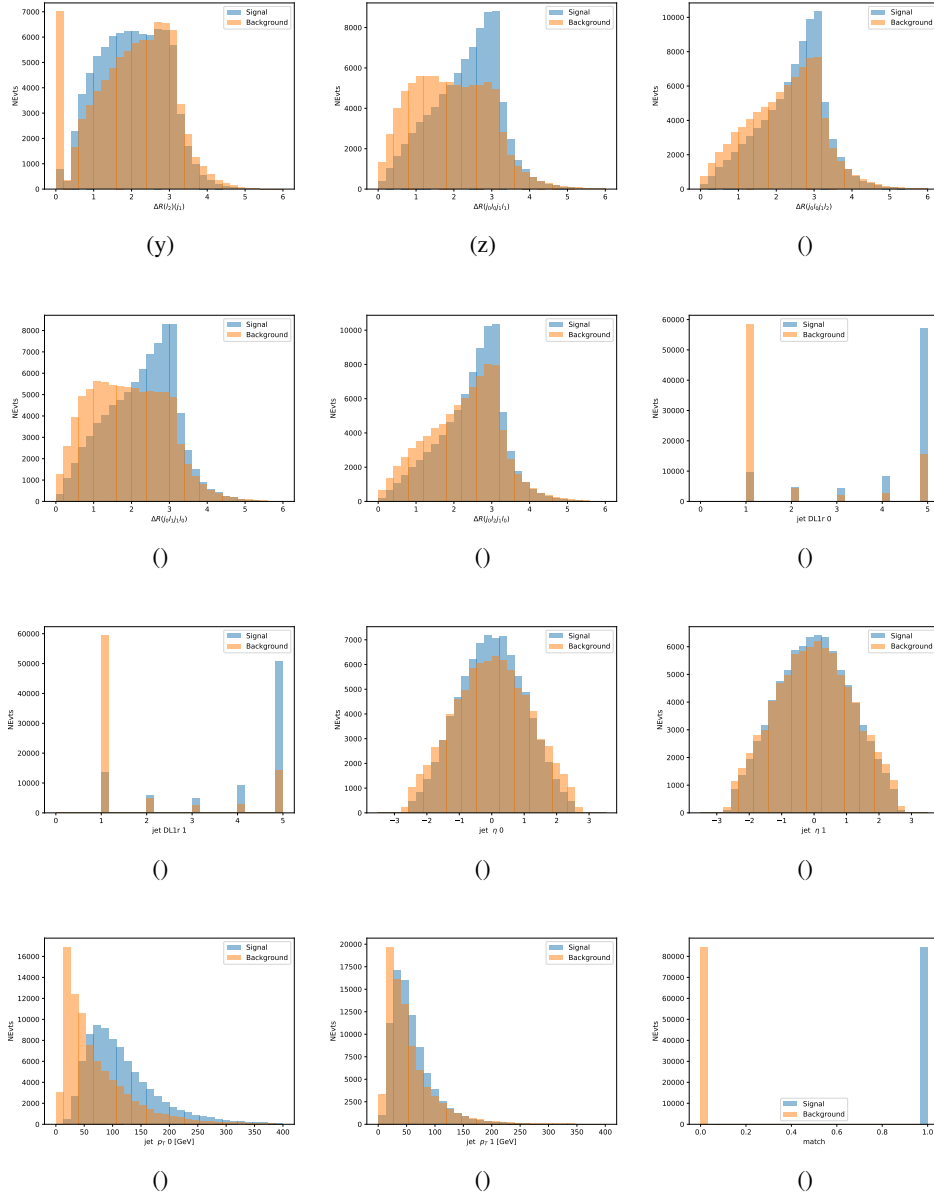
(v)



(w)



(x)



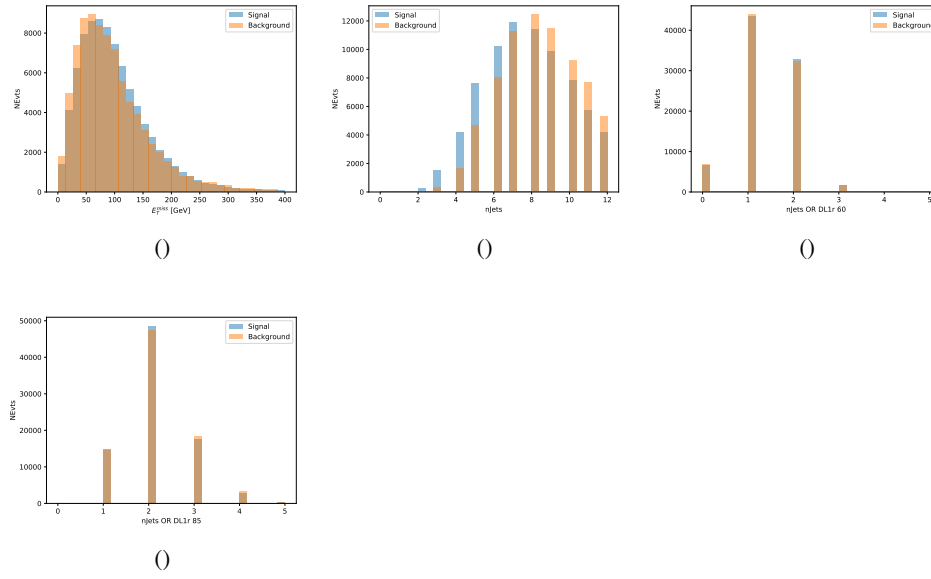


Figure 6.2: Input features for top3l training

7.1 Pre-MVA Event Selection

7.1.1 2lSS Channel

7.1.2 3l Channel

7.2 Event MVA

7.2.1 2lSS Channel

7.2.2 Semi-leptonic 3l Channel

7.2.3 Fully Leptonic 3l Channel

7.3 Signal Region Definitions

7.3.1 2lSS

7.3.2 3l

8 Systematic Uncertainties

The systematic uncertainties that are considered are summarized in table ???. These are implemented in the fit either as a normalization factors or as a shape variation or both in the signal and background estimations. The numerical impact of each of these uncertainties is outlined in section ???.

The uncertainty in the combined 2015+2016 integrated luminosity is derived from a calibration of the luminosity scale using x-y beam-separation scans performed in August 2015 and May 2016 [lumi].

The experimental uncertainties are related to the reconstruction and identification of light leptons and b-tagging of jets, and to the reconstruction of E_T^{miss} . The sources which contribute to the uncertainty in the jet energy scale [jes] are decomposed into uncorrelated components and treated as independent sources in the analysis.

The uncertainties in the b-tagging efficiencies measured in dedicated calibration analyses [btag_cal] are also decomposed into uncorrelated components. The large number of components for b-tagging is due to the calibration of the distribution of the BDT discriminant.

The systematic uncertainties associated with the signal and background processes are accounted for by varying the cross-section of each process within its uncertainty.

Table 2: Sources of systematic uncertainty considered in the analysis. Some of the systematic uncertainties are split into several components, as indicated by the number in the rightmost column.

Systematic uncertainty	Components
Luminosity	1
Pileup reweighting	1
Physics Objects	
Electron	6
Muon	15
Jet energy scale and resolution	28
Jet vertex fraction	1
Jet flavor tagging	131
E_T^{miss}	3
Total (Experimental)	186
Background Modeling	
Cross section	24
Renormalization and factorization scales	10
Parton shower and hadronization model	2
Shower tune	4
Total (Signal and background modeling)	40
Background Modeling	
Cross section	24
Renormalization and factorization scales	10
Parton shower and hadronization model	2
Shower tune	4
Total (Signal and background modeling)	40
Total (Overall)	226

9 Results

A maximum likelihood fit is performed simultaneously over the regions described in section ??.

Part I

Conclusion

As search for the effects of dimension-six operators on $t\bar{t}H$ production is performed. An effective field theory approach is used to parameterize the effects of high energy physics on the Higgs momentum spectrum. The momentum spectrum is reconstructed using various MVA techniques,

¹⁷² and the limits on dimension-six operators are limited to X.

173 **List of contributions**

174

175 **Appendices**

176 **A**